Geomorphology 106 (2009) 154–164

Contents lists available at ScienceDirect

Geomorphology

journal homepage: www.elsevier.com/locate/geomorph

Gravitational deformations and fillings of aging caves: The example of Qesem karst system, Israel

Amos Frumkin [a,*], Panagiotis Karkanas [b], Miryam Bar-Matthews [c], Ran Barkai [d], Avi Gopher [d], Ruth Shahack-Gross [e], Anton Vaks [c]

[a] Department of Geography, The Hebrew University of Jerusalem, Jerusalem, 91905, Israel
[b] Ephoreia of Palaeoanthropology–Speleology of Southern Greece, Arditou 34b, 11636 Athens, Greece
[c] Geological Survey of Israel, 30 Malchei Israel St., Jerusalem 95501, Israel
[d] Institute of Archaeology, Tel-Aviv University, Tel-Aviv 69978, Israel
[e] Institute of Archaeology, Bar-Ilan University, and Kimmel Center for Archaeological Science, Weizmann Institute of Science, Rehovot 76100, Israel

ARTICLE INFO

Article history:
Accepted 18 September 2008
Available online 7 October 2008

Keywords:
Cave fill
Speleothem
Cave archaeology
Karst subsidence
U–Th dating
Chamber cave

ABSTRACT

The Qesem karst system may serve as an example for aging chamber caves. It includes two caves which have undergone several stages of natural and human-induced deposition, as well as subsidence and collapse. Natural deposits include calcite speleothems, bedrock collapse debris, and clay fill. Karst dissolution and associated sagging and decomposition have operated since the initial cave formation. Inclined sediments are attributed to several processes, mostly dominated by gravitational sagging into underlying dissolution voids, affecting cave deposits and sometimes the host-rock. U–Th dating shows that speleothem deposition has been common during the mid-late Quaternary, but deposition sites shifted according to local conditions. The aging of caves occurs when they become totally filled by sediments and ultimately consumed by surface denudation, as documented in Qesem Cave.

1. Introduction

Deposits in prehistoric caves are often inclined or deformed (Garrod and Bate, 1937; Jelinek et al., 1973; Rapp and Hill, 1998). Understanding the deformation process is essential for interpreting archaeological finds and site-formation processes. The mechanisms of deformation often remain open questions, because of insufficient exposure or access. Low-energy sites, such as the southern Levant caves, commonly lack high-energy physical mechanisms, such as underground river flow. Gravity fall and colluvium for larger particles, sheetwash and wind for silt- and clay-size particles, are often the main agents inserting allochthonous sediments into the cave (Macphail and Goldberg, 1995; Gillieson, 2004; Goldberg and Sherwood, 2006). Under low-energy conditions, the deformation processes are often relatively slow. In order to elucidate the causes of observed structures, and their association with anthropogenic remains, close examination of the deformed site is needed, preferably using well-exposed field sections.

The Qesem karst system is a unique site in which natural and anthropogenic effects combine, with various types of deformation (Fig. 1). These are well exposed along natural outcrops, underground voids, and a roadcut which intersects the sediment-filled Qesem Cave (Barkai et al., 2003). This cave has a well-preserved archaeological sequence, dated to the end of the Lower Paleolithic period, which sheds light on the unique Acheulo–Yabrudian cultural complex in the Levant. Its rich anthropogenic deposits allow for a long-term field project, carried on since the cave was discovered in the year 2000 (Barkai et al., 2005; Gopher et al., 2005, Karkanas et al., 2007). Speleological processes are mostly inactive at Qesem Cave today, but are still active in the neighboring Kafr Qasem Cave where they have been documented for the last 25 years (Gasic, 2002). This allows for a detailed geomorphological study of the system, supported by dated speleothems, archaeological finds, speleological exploration and drilled cores.

In this paper the processes of cave filling and gravitational deformation are discussed according to the evidence of the surrounding karst system, including the active Kafr Qasem Cave and the inactive Qesem Cave, as well as other relevant sites in the region. This geomorphological study may help interpreting the anthropogenic

* Corresponding author.
E-mail addresses: msamos@mscc.huji.ac.il (A. Frumkin), pkarkanas@hua.gr (P. Karkanas), matthews@mail.gsi.gov.il (M. Bar-Matthews), barkaran@post.tau.ac.il (R. Barkai), agopher@post.tau.ac.il (A. Gopher), ruti@wisemail.weizmann.ac.il (R. Shahack-Gross), antonv@mail.gsi.gov.il (A. Vaks).

0169-555X/$ – see front matter © 2008 Elsevier B.V. All rights reserved.
doi:10.1016/j.geomorph.2008.09.018

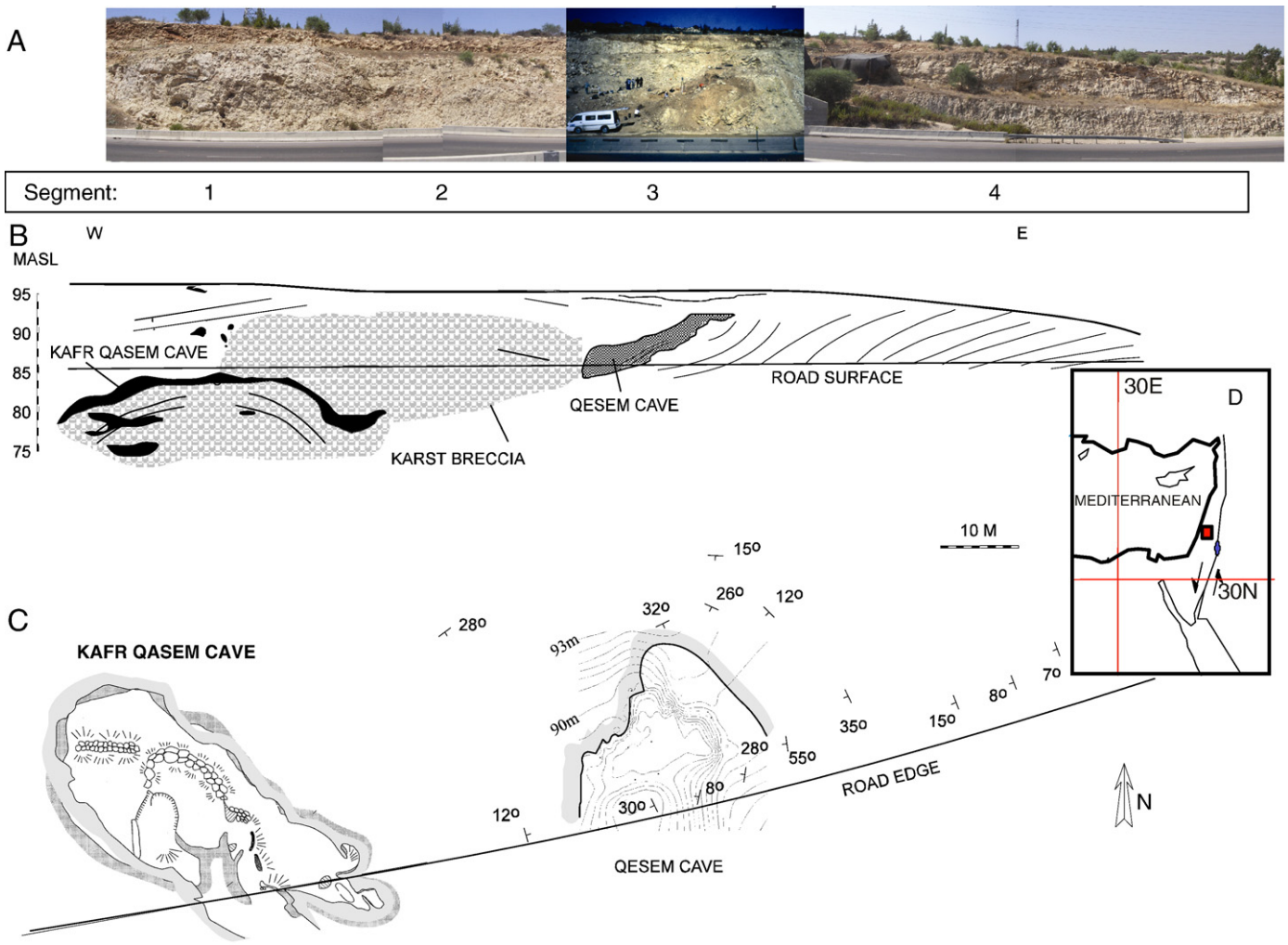

Fig. 1. Several views of the Qesem karst system. (A) Panorama of the roadcut with segment division. Photographs were taken in 2005. The central one, taken in 2001, shows Qesem Cave prior to the construction of its defensive fence and roof. The roadcut consists of 1–3 artificial steps. (B) Drawn section along the roadcut, with open cavities (black) and the remaining sediments of the filled Qesem Cave (gray). Black lines show measured inclinations within bedrock and sediments. (C) Horizontal projection (map) of the study site. Kafr Qasem Cave main features are shown as discovered on early 1980s. Altitude of the top sediments of Qesem Cave is shown (m above sea level), as in 2001. Measured bedrock dip is given in degrees. (D) Site location.

remains and human use in the cave (cfr. Karkanas et al., 2007), and possibly in other sites too.

1.1. Regional setting

The Qesem karst system comprises two chamber caves, ~40 m apart: the Qesem Cave archaeological site, and Kafr Qasem Cave, as well as their surrounding karstified rocks, all in the same geological context (Fig. 1). The whole system was observed and studied after being truncated by road construction works, since the 1980s.

The two caves are similar in origin, but they experienced different later histories.

Both caves are isolated chambers with no evidence of an underground stream. The Qesem karst system is located within a facing southward, 10° slope, 35 m above the nearby wadi stream bed. It has therefore not been affected by surface streams during the mid-late Pleistocene. The site is close to the border between the Samaria hills and the coastal plain of Israel, 90 m above sea level (Fig. 1), and ~70 m above the modern phreatic watertable. The phreatic aquifer drains westward, where its largest natural outlet, Rosh Ha'ayin Spring, is less than 6 km west of the Qesem karst system.

Local bedrock is Turonian limestone of Bi'na Formation (Hildebrand-Mittlefehldt, 1993), formed in an epicontinental shallow sea (Sass and Bein, 1978). The formation is generally thickly bedded, gently dipping westward and frequently karstified. Within the carbonate rocks of Israel, the Bi'na Formation is the richest in caves, with over 1000 caves in the backbone mountain ridge (Fischhendler, 1998; Frumkin, 2001; Frumkin and Fischhendler, 2005; Frumkin and Gvirtzman, 2006). High hydraulic conductivity of the local vadose zone was demonstrated by a groundwater contamination event through karstic voids, two km NW of the studied site (Avisar et al., 1997).

The Qesem region and the Samaria hills in general are rich in isolated chamber caves, whose most common feature is a single chamber with phreatic morphology (Frumkin, 1996; Frumkin and Fischhendler, 2005). The size of the chamber is commonly 10–30 m, while the largest is Atarot Cave, 35 km SE of Qesem Cave, measuring 203 m over 146 m. Such chamber caves are common at the unconfined zone of the mountain aquifer of Israel. Many such caves are believed to be associated with a past phreatic watertable, where concentrated downward-flowing vadose water mixes with the main groundwater body, renewing the aggressivity and dissolution. After the late

Table 1
U–Th dating results of stalagmites in Kafr Qasem Cave

Lab number	Remarks	Lamina	Age alpha (kyr)	$^{234}U/^{238}U$ (±1σ)	$^{230}Th/^{234}U$ (±1σ)	$^{230}Th/^{232}Th$	U (ppb)
	Stalagmite KK-1						
30A	Section along the growth axis	KK-1-A1	<1.2	1.079±0.054	0.001±0.011	Low ^{230}Th [a]	271
30B		KK-1-A3	3.17±1.62	1.078±0.041	0.029±0.015	Low ^{230}Th [a]	262
30C		KK-1-A4	37.88±2.17	1.115±0.031	0.296±0.013	385	456
31A		KK-1-A7	46.45±3.95	1.112±0.027	0.350±0.024	86	604
30D		KK-1-A9	55.13±5.54	1.089±0.029	0.400±0.030	16	409
33C		KK-1-A-11	60.08±3.13	1.087±0.021	0.427±0.016	1000	1247
31B		KK-1-A13	54.92±2.89	1.134±0.032	0.400±0.016	370	543
35C		KK-1-A14(I) [b]	61.76±3.83	1.044±0.022	0.4348±0.0192	476	396
35D		KK-1-A14(II) [b]	73.01±10.05	1.092±0.035	0.4930±0.0466	>170	377
27B		KK-1-B	63.1±4.9	1.087±0.043	0.433±0.024	>100	395
545A	Stalagmite KK-1	KK-1-A	49.15±5.04	1.061±0.049	0.365±0.029	95	536
553A	Section perpendicular to the growth axis	KK-1-C	52.99±4.57	1.117±0.057	0.389±0.025	163	579
545B	Stalagmite KK-2	KK-2-A	155.3±19.1	1.086±0.033	0.772±0.039	142	443
	Outer lamina						

The dates are uncorrected for detrital Thorium.
[a] ^{230}Th is too low and alpha spectrometry analytical uncertainty is too high for estimation of reliable $^{230}Th/^{232}Th$ ratios. These dates are used only as a general indication for the deposition period.
[b] Sample KK-1-A14 was dated twice.

Cenozoic regional uplift the caves were dewatered, initiating vadose processes. Ultimately, the exposed caves were truncated by subaerial erosion or human activity, while others probably remain hidden underground.

While caves appear in some localities, wide scale karstification is normally mostly effective at the epikarst — the upper few meters of the bedrock–soil interface. On the surface of the Qesem karst system, shallow pockets of *terra rossa* soil appear among massive residual blocks of karstified rocks. The *terra rossa* is composed mainly of clay minerals and quartz grains with lower content of calcite and dolomite. The mineralogy and isotopic composition indicates a high contribution of desert dust particles, rather than bedrock insoluble residue (Yaalon and Ganor, 1973).

2. Methods

The three-dimensional structure of the cave system is observed and measured in several views: (1) The natural truncation surface, particularly the Qesem Cave at the eastern part of the system; (2) Recent artificial roadcut of Israel route no. 5, transecting the karst system from east to west; (3) A series of five boreholes penetrating down to 11 m below road surface; (4) Speleological survey of the Kafr Qasem Cave; (5) Archaeological excavation uncovering the filling of Qesem Cave.

The macromorphology was measured using 'Disto' laser distance meter, inclinometer, compass, and horizontal photography. These were utilized both on the surface and inside the cave.

Bedrock and sediments were carefully measured and described in the field. Sediment and soil micromorphology was studied in thin sections using a stereomicroscope and a polarized light microscope (Karkanas et al., 2007).

The time frame of deposition, subsidence, and cave filling during the last 400 kyr is based on standard U–Th dating of speleothems. Preliminary dates by alpha spectrometry were performed at the Israel Geological Survey (Table 1). The preliminary chronology of Qesem Cave is based on TIMS dates, performed at the University of Bergen, and published earlier (Barkai et al., 2003). The chronology is further supported by the rich archaeological remains excavated in Qesem Cave attributed to the Acheulo–Yabrudian cultural complex of the terminal Lower Paleolithic period (Barkai et al., 2005; Gopher et al., 2005).

3. Results: Bedrock, karst and sediments

Bedrock in the study area is thickly bedded, hard biomicrite limestone, with high secondary porosity along fractures, bedding planes and cavities.

For a detailed description, the study area is crudely divided below into four segments along the road transect from west to east (Fig. 1). The segments reflect the division to the main caves (Qesem and Kafr Qasem) and the neighboring roadcut outcrops.

3.1. Segment 1 — Kafr Qasem Cave

Kafr Qasem Cave, the largest void in the Qesem karst system, dominates this segment. It consists of an up to 3 m high vaulted

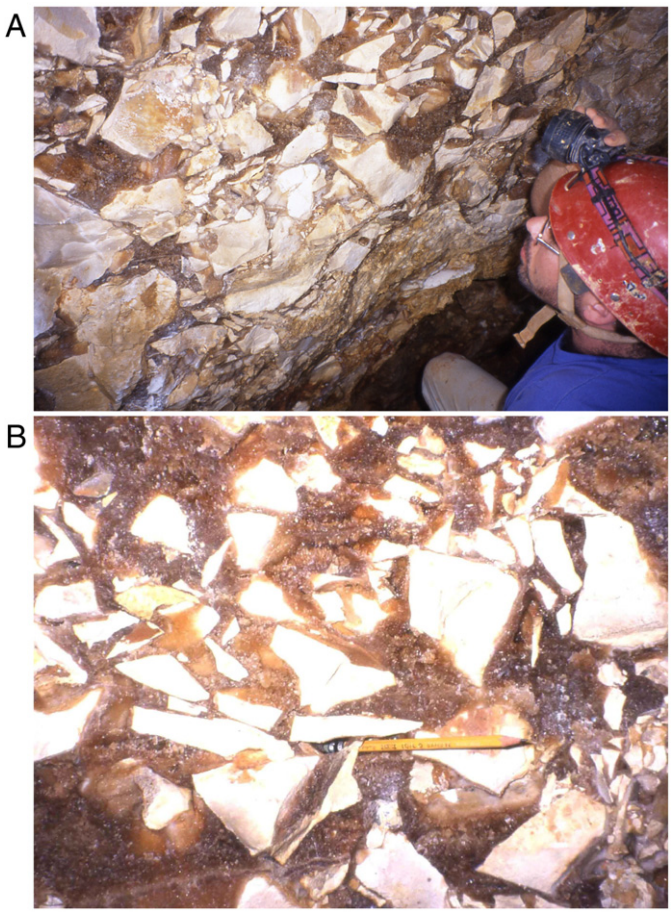

Fig. 2. Karstic breccia composed of angular limestone fragments, supported and lithified by speleothem calcite. (A) Inside Kafr Qasem Cave. (B) At the eastern side of Qesem Cave.

chamber, 40×17 m in size, oriented to NW. It is a simple case of natural chamber cave with no natural human-sized entrance.

The cave became accessible when it was breached by road construction during the early 1980s. In the last decade its southern end was removed by further construction works, but its present description refers to the original void. The cave is below the level of road surface, and is entered today via an artificial manhole at the road shoulder. The roadcut (Fig. 1A, B) exposed several small karstic voids above Kafr Qasem Cave, whose size commonly varies from 1 cm up to 1 m. The roadcut surface also exposed karstified, weathered bedrock above the cave. At the western part of the segment the bedrock dip is ~10° westward. At the eastern part of the segment the bedrock dip is hardly observed due to intensive fragmentation, forming unconsolidated or partly-consolidated karst breccia. The breccia, both here and within Kafr Qasem Cave, comprises angular rock fragments, often cemented by speleothem calcite (Fig. 2).

The cave ceiling is dominated by breakdown surfaces, rather than dissolution forms. The floor of the cave consists of unconsolidated rocks and cave deposits, forming a dome-shaped debris pile, roughly parallel to the cave ceiling. The peripheral parts of the debris pile slope outwards by up to 40°. The debris consists of unsorted crude blocks of bedrock, with some interstitial *terra-rossa* type clay. Close to the walls of the cave, mass movement and deformation, such as debris flow, slumping, rock fall and shattering, are common. These processes result in chaotic appearance of some sediments along the walls of the cave, where the chamber tapers obliquely downwards. Some indurated karstic breccia adheres to the ceiling and walls, suggesting several stages of deposition, deformation, fracturing and subsidence. The central part of the cave chamber is relatively horizontal. Here the debris pile is higher than in the peripheral zone. The debris pile has already reached the ceiling in some parts of the cave chamber, hardly allowing any additional collapse or mass movement there.

Water dripping is common in Kafr Qasem Cave from November through July (Gasic, 2002), indicating a temporary storage in the epikarst and upper vadose zone, which is practically drained at the beginning of the dry Mediterranean summer. The cave is wet especially along its south-eastern side, with active speleothems, including dripstone and pool deposits within a perched water-filled depression, 1×3 m in size, and 0.3 m deep. Dripstones covered by pool deposits and vice-versa indicate fluctuating pool water levels. The speleothems are of the types common in limestone caves, mainly composed of calcite with minor aragonite. Their stable position and growth trend indicates no severe deformation or subsidence during their deposition period.

The material underlying the cave floor was studied in a series of cored drillholes along the road at the southern end of the cave (Fig. 3).

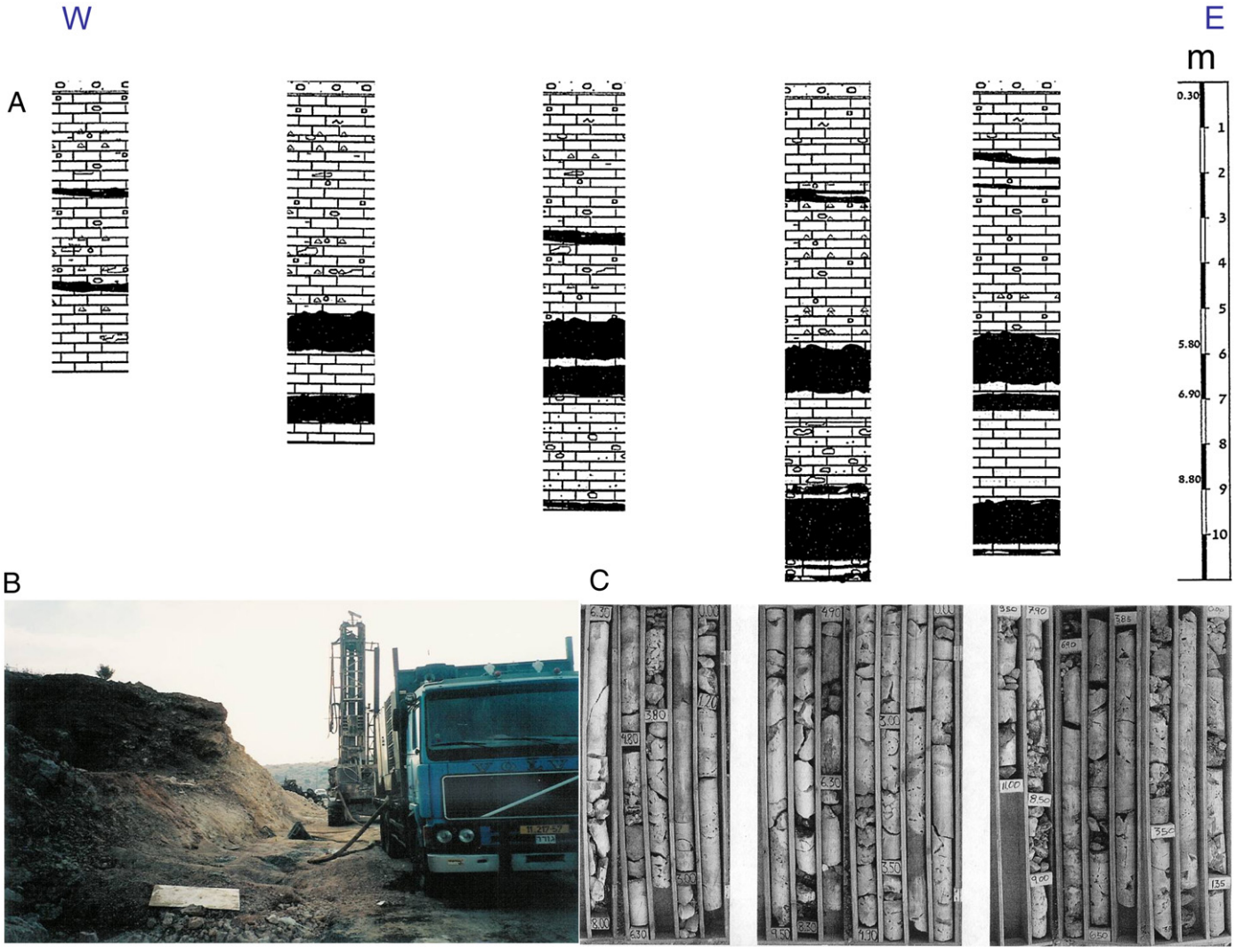

Fig. 3. Drilling under the road surface across segment 1 (Kafr Qasem Cave). (A) Five cores showing several voids (black) and abundant karstic breccia (vertical scale in meters). (B) The drilling rig. (C) Photograph of drilled cores, showing highly karstified limestone and karst breccia.

Fig. 4. Qesem Cave as truncated by roadcut, at the onset of archaeological excavations (2001). Dotted line indicates the approximate border between bedrock and cave sediments.

All voids, indicated by free fall of the drill, were carefully recorded. It was found that the material mainly comprises unconsolidated karstified rocks. Karstic voids are common, reaching an internal height of 1.5 m in two main levels under the explorable cave, and >20% in volume. Cores obtained from other parts of the drill holes are dominated by clast-supported karst breccia, with voids volume reaching up to 40%. In some cases the breccia is matrix-supported.

3.2. Segment 2

This segment consists of highly karstified limestone and karst breccia (Fig. 1B). In places, the rock is solid enough to distinguish the original massive beds, dipping ~12° to ENE (Fig. 1C). However, most of the limestone bedrock is highly weathered and fragmented, so bedding dip is hardly observed. The breccia is rarely clast-supported

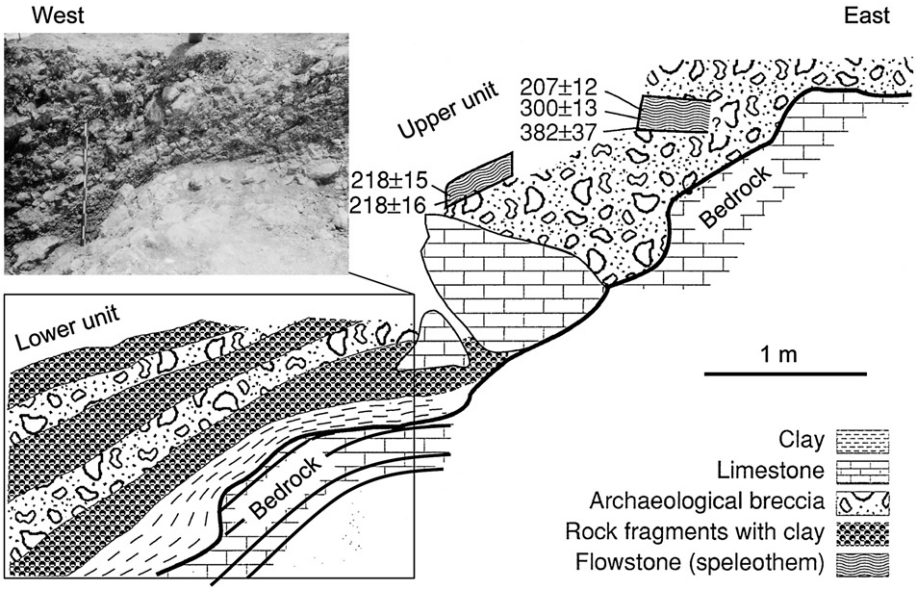

Fig. 5. Schematic section showing main field relations and dates at Qesem Cave. The lower sedimentary unit is inclined sub-parallel to the underlying bedrock layers. Limestone blocks within the cave sediments are attributed to collapse and subsidence. Bar in picture is 1 m long. Speleothem U–Th dates which fall within the section are given with standard deviation (in kyr), after (Barkai et al., 2003). Younger speleothems were dated in other parts of the cave.

Fig. 6. Qesem Cave sediments. (A) the main sedimentary section, looking eastward. The lower unit is below the feet of the person. Large collapsed boulders appear to the left of the person, at the bottom of the upper unit. (B) The upper sedimentary unit, exposed in its eastern side. Unstratified lithified calcareous archaeological deposits dominate the section, with limestone blocks embedded in the bottom, and thick flowstone termed Q3 close to the top. (C) The top of the upper sedimentary unit in Qesem Cave. Limestone blocks, attributed to roof collapse, are emplaced within calcified, shattered sediments. (D) Calcite flowstone, ~0.5 m thick, (Q3 of B), deposited in the upper part of Qesem Cave since ~382 kyr (see also Fig. 5, top right). Lithified calcareous archaeological deposit is observed below and above the flowstone. Human foot is for scale.

and comprises heterogenic angular limestone fragments, from ~1 mm to 1 m in size. The fragments are partly cemented by a matrix of speleothemic micrite to sparite calcite, (Fig. 2). Red iron-rich staining is common, associated with intruding *terra rossa* type clays from the surface, along fractures and karst voids.

3.3. Segment 3 — Qesem Cave

Qesem Cave is a sediment-filled chamber cave, discovered in 2000 when road construction works cut through its southern and upper parts (Fig. 4). The chamber is ~20×15 m in size and ~10 m high, although the exact dimensions of the cave awaits further field investigations. Massive limestone bedrock is exposed west, north and east of the cave, while on the south side the roadcut has removed the bedrock wall, and exposed a major part of the stratigraphic sequence of both cave sediments and surrounding bedrock. Archaeological excavation has exposed ~8 m thick archaeological deposits containing rich faunal and lithic assemblages.

The lithic industrial sequence of the cave is blade-dominated (Barkai et al., 2005; Gopher et al., 2005) and attributed to the Amudian industry of the Acheulo–Yabrudian complex at the terminal Lower Paleolithic period (late Middle Pleistocene). The Acheulo–Yabrudian cultural complex postdates the Acheulian culture of the Lower Palaeolithic period and predates the Mousterian culture of the Middle Palaeolithic period, and it correlates with Jelinek's "Mugharan Tradition" (Jelinek, 1990).

A distinct feature of the surrounding bedrock is its centripetal dip towards the cave chamber. The bedding dip increases towards the cave void, reaching up to 55° (westward) at the eastern wall of the cave (Fig. 1C). The dip reaches 32° (to SSE) at the northern side of the cave, and 12° (eastward) at the western wall of the cave. Considering the general westward dip in the region, the deformation at the western side is in the same order of magnitude as at the northern and eastern sides. The deformed bedrock is associated with ubiquitous fracturing and brecciation. The breccia on the western side of the cave wall is often cemented by secondary calcite spar matrix, while on the eastern side the fragmented bedrock is crumbling. The bedrock at the northern side of the cave is less commonly fractured, but it shows dissolution weathering along the few fractures, with some speleothems in widened fractures which became small voids.

The Qesem Cave deposits were divided into two major stratigraphic units (Karkanas et al., 2007). The lower unit was excavated a few meters west and south of the upper unit (Figs. 5 and 6), while a physical connection between the two units was initiated during the 2006 excavation season.

3.3.1. Lower unit

The lower unit consists of westward-inclined layers of predominantly limestone fragments interspersed with clay, all containing archaeological finds. The inclination of the sediments is sub-parallel with the apparent dip of the underlying bedrock (Fig. 5). The lowermost part of the unit is ~half a meter of reddish brown clay that is gradually enriched in larger clasts from bottom to top, with alternations of clay and coarse limestone fragments. The fine sediments contain mainly reddish brown clay, with small amounts of fine sand-size quartz, and some silt. Black iron–manganese staining,

as well as black layers are common. Some small open voids have been observed at the lowermost excavated level, below the bottom layers of Qesem cave.

In the lower unit anthropogenic remains are commonly observed. Small bone fragments within the clay are subangular to subrounded, and sand to silt sized. The uppermost meter of the lower unit consists of clast-supported limestone fragments; some are 20–30 cm long and even larger, with some interstitial clay. The limestone blocks indicate physical decomposition of the cave roof or walls. The limestone fragments are sub-rounded and form inclined horizons. The inclination gradually decreases upward within the lower unit. The clastic layers contain gravel-sized bone fragments. Black crust-like surfaces and weak sorting, possibly by water or slumping, enhance the stratification.

3.3.2. Upper unit

The stratification of this unit is less clear, and it is less inclined than the lower one. It has been deposited mostly after the lower unit had stabilized, as attested by the upward-decreasing inclination of the lower unit. The upper unit is mostly exposed as an artificial escarpment on the eastern side of the cave. Its lower part is rich in limestone blocks embedded in lithified calcareous deposit, light reddish brown in color (Fig. 6A). Some of the limestone blocks are very large ~1–1.5 m long, mostly at the contact area between the lower and upper units. These blocks indicate a large collapse event that significantly transformed the cave structure and probably enlarged its entrance.

The sediment was intensively fractured after cementation in most parts of the upper unit, mainly along the cave walls. These fractures have been filled later by debris. Some original stratification is still visible locally. Secondary calcite cementation of the deposits, as well as speleothems, is common close to the eastern wall of the cave. Sediment type differs with its proximity to the bedrock walls of the cave, as described below.

Away from the walls, the upper unit is composed of a small fraction of limestone clasts cemented calcareous matrix, mostly horizontally bedded. The coarse material consists predominantly of gravel sized sub-rounded limestone and angular bone fragments. The matrix consists of micritic to microsparitic calcite, dotted with oxidized red aggregated or dispersed clay. Wood ash and burning remnants are common (Karkanas et al., 2007). Calcified rootlets are commonly observed in this unit, in the form of numerous small bifurcating channels cemented with calcite.

The deposits closest to the walls are relatively less stratified. Close to the former north wall of the cave the sediment is more shattered than in areas close to the former south wall. Bedding is less clearly defined and the sediments contain relatively large amounts of infiltrated clay in the form of moderately cemented patches of orange–red calcareous clay. The sediment is heterogeneous, disturbed and cemented by massive micritic calcite. Several generations of veins of the same massive micrite cross-cut the matrix. Erosional surfaces are common, as are sheared contacts lined with striated clay on already consolidated material. More recent non-cemented shattered areas are also found. Within the lower part of the upper unit, in at least one area, is a one-meter thick archaeological layer with very soft sediments which is very rich in finds. This layer is trapped between two cemented layers and was covered by a 20 cm thick cemented crust. As the crust was removed during the excavation, a rich layer with very soft sediments was reached. Within this layer some horizontal finds concentrations are of note.

Some large bone fragments have almost vertical or inclined orientations. Shattering was a common process, which continuously modified the sediments. Calcified rootlets are also observed, contemporaneous with the main cementation and fissuring processes. Limestone fragments become more abundant at the top of the upper unit (Fig. 6B–C), probably associated with additional collapse of the cave roof.

Several bedrock fragments found in several locations at the topmost part of the upper sequence have been analyzed using infrared spectrometry and their mineralogy was determined. Four out of ca. 10 rock fragments are composed of dolomite, either exclusively or together with calcite. The rock fragments are not retouched/shaped, i.e., they can be regarded as natural “fieldstones”. Therefore, they may have been either brought to the cave by its inhabitants or entered through the entrance by gravitational and/or water action from above.

Some large (~1 m size) limestone blocks are also found, not very different than the ones at the contact area between the lower/upper units (Fig. 6C, lower left corner). These indicate another large collapse event, possibly associated with the terminal existence of the cave void.

Much of the Qesem Cave sediments consist of lithified ash remains, sometimes preserving intact hearths (Karkanas et al., 2007). This indicated that physical deformation is rather local. A large part of the sediments are generally still *in situ* or only slightly displaced. The most common deformation in Qesem Cave is physical, produced by mechanical movement and shattering of some sediments. Chemical alteration and diagenesis in acidic conditions are relatively rare compared to other prehistoric caves in the region, allowing for good preservation of ash and bones (Karkanas et al., 2000; Shahack-Gross et al., 2004). On the other hand, siliceous materials such as basalt fragments are severely damaged chemically due to the highly alkaline conditions in the cave (Karkanas et al., 2007).

Speleothems in Qesem Cave are less common than in Kafr Qasem Cave. They are observed mainly in the upper unit close to the eastern wall of the cave. They comprise a thick (~0.5 m) flowstone layer (Q3, Fig. 6D), calcite crusts, and small dripstone deposits. Speleothem calcite also comprises the matrix of most karst breccia around the cave. The speleothems are coarsely crystalline to micritic, indicating deposition within a sheltered cave, rather than close to a cave entrance. Most of the speleothems and veins are also fragmented and secondarily cemented. Clay-supported rounded speleothem granules were incorporated into younger generation speleothems.

3.4. Segment 4

This segment, particularly at its eastern side, is less-affected by karstification and deformation processes compared to the other segments. Therefore it can serve as a ‘control group’ for comparison with the other, more deformed segments.

East of Qesem Cave the deformation and karstic features are fading across some fifty m. Bedrock is well bedded to massively bedded. Bedrock generally dips to the west; the inclinations decrease gradually from west to east, from 55° near Qesem Cave, to 7° in the eastern side of the segment (Fig. 1B–C). Bedrock fracturing and karstification is very intense close to Qesem Cave, rapidly decreasing eastward. The fractures and small karstic voids are commonly filled with brown-reddish clay, and partly with speleothem calcite. In the eastern portion of segment 4, karst weathering becomes restricted to the epikarst — the uppermost 1–2 m of the bedrock mass. In general, bedrock features in the eastern part of the segment are similar to the regional unkarstified areas in dip, fracturing and karstification.

3.5. Dating

U–Th dating of speleothems (Table 1) was performed in the larger cave voids of segment 1 (Kafr Qasem Cave) and segment 3 (Qesem Cave). The relative stratigraphic position of the dated sediments provides the general chronology of the karst system, albeit within the dating limit of ~400,000 years. Correction for detrital thorium was not performed for the present study, because only the general chronological framework is considered here.

Kafr Qasem Cave dates range from ~155,000 years to today (Table 1). In spite of the sampling bias (particularly towards relatively

recent deposits), the available dates fall in the previous glacial, last glacial, and present interglacial periods. Most of the dated samples fall during marine isotopic stages 4 and 2 of the last glacial period, but further sampling may show additional deposition periods, in particular older dates, as observed in stalagmite KK2 whose outer lamina is 155,000 years old. The speleothems are still active within several parts of the cave, particularly in the eastern side. Most of the observed deposition took place within the present form of the cave void, after most of the collapse occurred. Older speleothems are mainly observed within the sediments and karstic breccia. The dated Qesem Cave speleothems have been deposited mostly from ~400,000 to ~150,000 years ago, with only slight later deposition which was not studied here (unlike Kafr Qasem Cave, where deposition has been active later). The bottom- to middle layers of the thick flowstone (Q3) located at the upper part of the upper sequence (Fig. 6D) dates between ~382 and 207 kyr (Fig. 5; Barkai et al., 2003). Micromorphological analysis of the upper layer of Q3 shows clear signs of dissolution and re-precipitation of calcite, so it could not be dated. The uppermost 0.5–1.0 mm includes clay and also possibly phosphates. In the 2–3 cm below, the calcite crystals appear in a vertical, dendritic-like form, and many microscopic dissolution voids are present in this calcitic mass. Only the middle and lower calcitic bands below seem intact and do not include dissolution voids, so they could be dated.

Acheulo–Yabrudian sediments have been calcified, fractured and then covered by a thin speleothem crust dated to 152,000 years. The Acheulo–Yabrudian occupation in Qesem Cave ceased long before that date, probably around ~200,000 years ago (Barkai et al., 2003). Only slight deposition occurred during the last glacial period, and apparently no deposition during the Holocene. Speleothem dates later than 200,000 years seem not to be directly associated with anthropogenic activity, but rather with later karstic deposition.

4. Discussion

The Qesem karst system displays several modes of development associated with different spatial conditions and history of each segment. The local conditions affected the deformation geometry of each segment.

4.1. Subsidence associated with weathering zones

Deep weathering zones and “archaeological breccia” are dominant features in Qesem karst system. Scattered voids induce an overall gravitational subsidence and compaction. The dip of the fragmented, weathered rock is controlled by local variations in weathering, associated with solution rates and fracture pattern. The original structure of the bedrock is retained in some places, but in others the brecciated rock becomes chaotic in appearance. These processes are very common in the segments 1–3 of the Qesem karst system. The details of each segment are discussed below.

4.2. Collapse dome — Kafr Qasem Cave

Kafr Qasem Cave demonstrates a convex-upward cross section (Fig. 1B) with breakdown debris on the floor, punctuated by relatively small voids. This form is a consequence of a long term mechanical failure of the cave roof. The collapsed void developed a tension dome in its roof. The dome shape is the most efficient in distributing the stress of the remaining bedrock (White and White, 2000). There is no underground stream which could remove the talus pile. The previously tightly-packed bedrock accumulated as a pile on the cave floor in a less compact order, causing the remaining void to migrate upwards and diminish in volume [a process termed stoping (Ford and Williams, 2007)]. The weight of the remaining roof is transferred to the cave walls surrounding the tension dome. Speleothems deposited in the void in its present form indicate that the collapse process may have stabilized during the last glacial cycle. However, this is only quasi-equilibrium, as collapse may continue due to surface denudation, earthquakes and dissolution along fractures or bedding planes, until the void is eliminated. Further collapse would destroy or cover the existing speleothems, which would later be replaced by new deposition in the future quasi-equilibrated void. The debris pile on the cave floor attained a shape of a convex-upward dome, similar to the form of the roof stress dome. The debris material on the floor is horizontally bedded in the center of the void, becoming more inclined outwards close to the walls, around the perimeter of the void. At the extreme boundary of the chamber, the void tapers to widened, inclined fractures, where sagging of the floor has been relatively small.

Two processes tend to fill the cave chamber, before it is breached by surface denudation: (1) volumetric decrease of the remaining void due to collapse and reorientation of blocks in the debris pile; (2) deposition of speleothems and clay sediments. When the chamber is small enough, like in Kafr Qasem Cave it would ultimately reach the surface as a breccia pipe rather than an open void (Ford and Williams, 2007).

4.3. Gravitational sagging of bedrock and sediments

Qesem Cave combines several gravitational effects which deform various kinds of sediments during a lengthy period under changing conditions. The question arises, if the inclination of the lower unit beds is original (tectonic) or secondary, associated with a later deformation.

The following observations are relevant to this question:

(1) The bedrock in the vicinity of Qesem Cave dips towards the center of the cave (Fig. 1B–C).
(2) The bedrock dips are largest at the eastern wall of Qesem Cave reaching 55°. The dip becomes smaller with increasing distance from the cave wall. The larger dips are associated with increasing shattering of the rock, without chaotic displacement of rock fragments.
(3) As one moves eastward of Qesem Cave, the bedrock regains its original bedding and structure.
(4) The measured dips are not associated with any known tectonic stress field in the region (Bahat et al., 2006). They rather vary locally, and are generally directed in a centripetal way around Qesem Cave (Fig. 1B–C).
(5) The local bedrock dips cannot be attributed to a tectonic fault or fold, because these are not observed at the outcrops around the cave.
(6) The lower sedimentary unit in the cave is well-bedded, without chaotic appearance (Fig. 5).
(7) The inclined lower Qesem Cave deposits are sub-parallel with the underlying bedrock layers. Both are inclined considerably more than the regional bedrock dip.
(8) Steep inclinations of lower cave deposits are common in prehistoric caves, such as Tabun, where the inclined sediments lie on a funnel shaped bedrock surface (Garrod and Bate, 1937; Jelinek et al., 1973; Ronen and Tsatskin, 1995; Zviely and Ronen, 2004) and Kebara (Goldberg and Bar-Yosef, 1998). As in Qesem, the Kebara and Tabun deposits are mostly inclined in the lowermost sedimentary units (Tabun layers F and G).
(9) Similar bedrock deformation of short (~20 m) wavelength is common in Bi'na Formation between the Samaria hills and the coastal plain of Israel (Fig. 7). At least some of them can be attributed to underlying, hypogene dissolution below the water-table (Frumkin and Gvirtzman, 2006).

Several processes may contribute to the dip of cave sediments: initial dip of sediments deposited on an inclined bedrock floor of the cave; differential dissolution or other diagenetic modification of cave sediments; compaction of unconsolidated sediments; preferential dewatering of sediments, or volumetric expansion due to absorption

Fig. 7. Bedrock sagging structures in Bi'na Formation a quarry 22 km south of Qesem karst system. The sagging syncline is attributed to the underlying karstic voids, associated with hypogenic dissolution (Frumkin and Gvirtzman, 2006).

of water by clays. However, these processes cannot explain the deformation of the underlying *bedrock* layers in Qesem Cave. The most likely process in this case is an overall sagging of bedrock and sediments into underlying voids as happens in subsidence depressions (Ford and Williams, 2007). The subsidence, affecting both bedrock and cave deposits, must have occurred after the initial sedimentation within the cave and appears to be penecontemporaneous to sedimentation of the upper parts of the lower unit.

Sagged bedrock layers in segments 2 to 4 are locally inclined considerably more than the regional dip, but they generally retain their original volume. Similar inclined local structures are observed in several sites in the region. For example, a quarry 22 km south of Qesem displays bedrock sagging structures where underlying karstic voids are well exposed (Fig. 7). The evidence suggests gradual dissolution of bedrock under the deformed rock, promoting gradual sagging of overlying strata. The consequence is slight shattering and uniform sagging of the bedrock layers, together with the overlying cave sediments. The sagging beds are inclined towards the center of the underlying dissolution zone. A more rapid process can induce larger shear stresses and local rupture depending on the competence of the rock. The sagging is promoted by low-competence rock. Higher competence may lead to the development of a stress dome with possible gradual subsidence or catastrophic collapse.

4.4. Filling and further deformation of cave sediments

The initial sedimentation of clay in Qesem Cave occurred under wet conditions, indicated by black iron–manganese staining. The clay could seep with vadose infiltration from the subaerial *terra rossa* soil. Anthropogenic material, including fragmented bones and flint artifacts are found from the lowermost layers upward. This proves that during the initial deposition of the lower sediment unit, the cave already had an entrance from the surface, allowing hominids to use the cave, and associated anthropogenic material to accumulate. *Terra rossa* clay-type inclined deposits intermingled with rock fragments may indicate some gravitational penetration of surface material through an upper narrow entrance, which is common within chamber caves of the region. In Qesem Cave it includes gravitationally-moved large sized material and detritic sediment transferred by sheetwash.

The upward-increasing amount of limestone clasts in the lower unit probably originated from collapse and fragmentation within the cave, because the penetration of large blocks from the outside seems unlikely. Sand-sized quartz could originate from sand inclusions within the host bedrock or from surface late Cenozoic deposits.

The middle part of the lower sediment unit, as well as the overlying layers up to the top of the sequence, are rich in anthropogenic material, including bone and flint items, flint tools and wood ash remains (Karkanas et al., 2007).

Boulders in the lower part of the upper unit (Fig. 6A center) indicate collapse event(s) which probably originated from the cave walls and/or roof, and probably enlarged the cave entrance. This collapse must have changed dramatically the shape of the former cave. Calcified rootlets throughout the upper unit could indicate the initiation of plant growth within the open cave, although the roots can also be attributed to subaerial flora. Fractures within the lithified sediments along the cave walls probably resulted from pressure-release within the indurated sediments, with gravitational slumping of cemented blocks into the central void. This could occur by gradual enlargement of an underlying void, as well as further sagging, subsidence and compaction of the lower unit sediments. Microscopic erosional features, incorporation of small fragmented earlier sediments into newer ones, and several fracture generations, all indicate continuous or recurrent modification of the cave sediments by lithification, shattering, erosion, and subsidence.

Speleothems were deposited in the upper unit along the eastern wall between ~380,000 and 150,000 years ago. This indicates that until ~150,000 years ago the eastern part of the cave still had at least a few m thick roof, supporting normal epikarst with small fractures through which rainfall could infiltrate from the surficial *terra rossa* soil. Calcium-carbonate rich water also contributed to lithification of loose sediments, and penetrated fractures in the previously solidified debris pile, depositing calcite veins.

The calcite speleothems, cementation, and veins, as well as the preservation of bones, all indicate that the percolating water was

typically oversaturated with respect to calcite. This precluded intensive dissolution of the sediments.

It seems that the uppermost centimeters of the thick flowstone (Q3) have been subject to dissolution in antiquity, associated with possible re-opening of the U system, following its deposition. This dissolution might have resulted from a change in the chemistry of water, becoming undersaturated to calcite and thus aggressive. The change, in turn, can be a result of the removal of the soil cover, a climatic change (related to the soil cover status), open fractures that let the water flow without much interaction with the limestone, smaller thickness of the overhanging rock, or lack of a cave roof. These alternatives are classified to two possible scenarios: regional environmental change associated with erosion of the soil cover, or local changes in the configuration of Qesem Cave. The fact that deposition continued in the nearby Kafr Qasem Cave as well as other caves in the region (e.g. Frumkin et al., 1999) indicates that local changes controlled the deposition and dissolution in Qesem Cave. Dead speleothems now being dissolved are frequently found in caves of Israel, and they are not necessarily associated with regional environmental change. On the contrary, condensation corrosion of speleothems occurs in most caves of the region following the cessation of deposition.

The dating results show that ~150,000 years ago speleothem deposition diminished further in Qesem cave, and its final evolutional stage started. The cave probably became unroofed by collapse and surface denudation (for other examples see Klimchouk, 2006; Mihevc et al., 1998). Regional subaerial denudation rate is estimated ~15–40 m/Myr (Gerson, 1975; Haviv et al., 2006), so at least 10 m of denudation could occur since deposition started within the cave. The void became completely filled with sediments up to the hill surface and it ceased functioning as an active depositional site. Following the rich Acheulo–Yabrudian complex of the terminal Lower Paleolithic, no anthropogenic usage of the cave is observed during the last ~200,000 years. Speleothem deposition became limited to small voids and fractures (e.g. some small coralloid crusts).

5. Conclusions

Inclined and deformed cave sediments may be associated with depositional dip, subsidence and sagging into deeper voids, stoping and doming of cave roof, introduction of subaerial materials through an upper entrance, internal irregular accumulation and deformation processes, tectonic deformation, seismic tilting and collapse, diagenetic chemical processes, or gravitational compaction of loose sediments and dissolved material. Many of these processes are controlled by gravity. Some affect only the internal cave sediments, while some gravitational deformations affect the bedrock skeleton of the karst system as well. These processes usually affect the geometry, distribution and interpretation of archaeological finds, so they must be seriously analyzed. Allochthonous sediments are rare in the discussed region, and are mostly associated with wind, biological or anthropogenic agents when the cave has an entrance. These are well represented in the Qesem karst system which combines both natural karst processes and anthropogenic-modified sediments.

The Qesem Cave deposits are the most complex within the studied karst system. They contain a combination of natural and anthropogenic sediments, such as flint and bone fragments as well as ash-rich material. Subsidence, erosion, fracturing, deposition of various sediments and cementation were continuous or recurrent within Qesem cave, at least during the mid-Pleistocene. Qesem cave is a good example of the way karstic caves are filled and ultimately obliterated by surface denudation and roof collapse. These processes are considered as “aging” of a karstic cave.

The Qesem karst system has been an active depositional site for speleothems during the last glacial cycles, including both glacial and interglacial periods. In particular, the termination of speleothem deposition in Qesem Cave is not a regional trend, but a local effect, related to the aging of this particular cave. The continuous recent deposition is well documented in Kafr Qasem Cave and also in other caves of the region. Speleothem deposition at any particular site within the system depended on the supply of Ca-carbonate water which gained its solutes in the epikarst zone, above the deposition site.

About 150,000 years ago the epikarst layer was probably degraded or totally removed from the top of Qesem cave, so the cave void apparently ceased to operate as an active vadose zone depositional environment. This removal is associated with the denudation and collapse of the cave roof. This particular cave has ceased to operate as a depositional site, and is being actively consumed by surface erosion as well as anthropogenic impact. The cave aging processes discussed here are ubiquitous and relevant to most karstic systems.

It may be concluded that intrinsic, local causation of cave processes, such as deformation and speleothem deposition, may be more important than extrinsic, regional causation within the same climatic zone. This should not be overlooked by geoarchaeologists wanting to establish regional patterns.

Acknowledgements

Aaron Kaufman has initiated U–Th dating in Kafr Qasem Cave. The team of the Cave Research Unit at The Hebrew University of Jerusalem surveyed Kafr Qasem Cave. The study was supported by the Water Authority of Israel, the Israel Science Foundation (Grant No. 256/05), the L.S.B. Leakey Foundation (2003–2006), and the Irene Levi Sala CARE Archaeological Foundation (2003–2006).

References

Avisar, D., Kronfeld, J., Isa, A., 1997. The influence of cesspools in Arabs villages upon drinking water quality. The Ecoadvocate, Israel Union for Environmental Defence, 1997(winter), pp. 4–9.
Bahat, D., Frid, V., Rabinovich, A., 2006. Paleostress clockwise rotation in the Sinai–Israel sub-plate and the initiation of the Dead Sea Rift. Israel Journal of Earth Sciences 55, 159–171.
Barkai, R., Gopher, A., Lauritzen, S.E., Frumkin, A., 2003. Uranium series dates from Qesem Cave, Israel, and the end of the Lower Palaeolithic. Nature 423, 977–979.
Barkai, R., Gopher, A., Shimelmitz, R., 2005. Middle Pleistocene Blade Production in the Levant: An Amudian Assemblage from Qesem Cave, Israel. Eurasian Prehistory 3, 39–74.
Fischhendler, I., 1998. Factors Controlling the Karst Pattern in Southern Samaria (in Hebrew). MA Thesis, The Hebrew University, Jerusalem, 64 pp.
Ford, D.C., Williams, P.W., 2007. Karst Hydrogeology and Geomorphology. Wiley, Chichester. 562 pp.
Frumkin, A., 1996. Geology and speleology of Nahal Qanah Cave System. In: Gopher, A. (Ed.), The Nahal Qanah Cave. Institute of Archaeology Monograph Series. Tel Aviv University, Tel Aviv, pp. 139–146.
Frumkin, A., 2001. The Cave of the Letters sediments — indication of an early phase of the Dead Sea depression? The Journal of Geology 109, 79–90.
Frumkin, A., Fischhendler, I., 2005. Morphometry and distribution of isolated caves as a guide for phreatic and confined paleohydrological conditions. Geomorphology 67, 457–471.
Frumkin, A., Gvirtzman, H., 2006. Cross-formational rising groundwater at an artesian karstic basin: the Ayalon Saline Anomaly, Israel. Journal of Hydrology 318, 216–333.
Frumkin, A., Carmi, I., Gopher, A., Tsuk, T., Ford, D.C., Schwarcz, H.P., 1999. Holocene millenial-scale climatic cycle from Nahal Qanah Cave speleothem, Israel. The Holocene 9, 677–682.
Garrod, D.A.E., Bate, D.M.A., 1937. The Stone Age of Mount Carmel. Clarendon Press, Oxford.
Gasic, T., 2002. The Influence of Road Construction on Karst Systems. MA Thesis, Hebrew University, Jerusalem, 82 pp.
Gerson, R., 1975. Karst and fluvial denudation of carbonate terrains under sub-humid-Mediterranean and arid climates — principles, evaluation and rates (examples from Israel). In: Gams, I. (Ed.), Karst Processes and Relevant Landforms. University of Ljubljana, Ljubljana, pp. 71–79.
Gillieson, D., 2004. Sediments: allochthonous clastic. In: Gunn, J. (Ed.), Encyclopedia of Cave and Karst Science. Fitzroy Dearborn, New York, pp. 633–634.
Goldberg, P., Bar-Yosef, O., 1998. Site formation processes in Kebara and Hayonim Caves and their significance in Levantine prehistoric caves. In: Akazawa, T., Aoki, K., Bar-Yosef, O. (Eds.), Neandertals and Modern Humans in Western Asia. Plenum, New York, pp. 107–125.
Goldberg, P., Sherwood, S.C., 2006. Deciphering human prehistory through the geoarcheological study of cave sediments. Evolutionary Anthropology 15, 20–36.
Gopher, A., Barkai, R., Stiner, M.C., Shimelmitzi, R., Khalaily, M., Lemorini, C., Hershkovitz, I., 2005. Qesem Cave: an Amudian Site in Central Israel. Journal of The Israel Prehistoric Society 35, 69–92.

Haviv, I., Stone, J., Enzel, Y., Zilberman, E., Whipple, K., Matmon, A., Fifield, K., 2006. Climatic control on erosion rates of dolo-limestone hilltops. In: Kessel, R., Kagan, E., Porat, N. (Eds.), Annual Meeting. Israel Geological Society, Bet-Shean, p. 54.

Hildebrand-Mittlefehldt, N., 1993. Kefar-Sava. The Geological Survey of Israel, Jerusalem, p. 1.

Jelinek, A.J., 1990. The Amudian in the context of the Mugharan Tradition at the Tabun Cave (Mount Carmel), Israel. In: Mellars, P. (Ed.), The Emergence of Modern Humans. Cornell University Press, Ithaca.

Jelinek, A.J., Farrand, W.R., Haas, G., Horowitz, A., Goldberg, P., 1973. New excavations at the Tabun Cave, Mount Carmel, Israel, 1967–1972: a preliminary report. Paleorient 1, 151–181.

Karkanas, P., Bar-Yosef, O., Goldberg, P., Weiner, S., 2000. Diagenesis in prehistoric caves: the use of minerals that form *in situ* to assess the completeness of the archaeological record. Journal of Archaeological Science 27, 915–929.

Karkanas, P., Shahack-Gross, R., Ayalon, A., Bar-Matthews, M., Barkai, R., Frumkin, A., Gopher, A., Stiner, M.C., 2007. Evidence for habitual use of fire at the end of the Lower Paleolithic: site formation processes at Qesem Cave, Israel. Journal of Human Evolution 53, 197–212.

Klimchouk, A., 2006. Cave un-roofing as a large-scale geomorphic process. Speleogenesis and evolution of karst aquifers 4 (1), 11 www.speleogenesis.info.

Macphail, R.I., Goldberg, P., 1995. Recent advances in micromorphological interpretations of soils and sediments from archaeological sites. In: Barham, A.J., Macphail, R.I. (Eds.), Archaeological Sediments and Soils: Analysis, Interpretation, and Management. Institute of Archaeology, University College London, London, pp. 1–24.

Mihevc, A., Slabe, T., Sebela, S., 1998. Denuded caves — an inherited element in the karst morphology; the case from Kras. Acta Carsologica 27, 165–174.

Rapp, G.J., Hill, C.H., 1998. Geoarchaeology. Yale University Press, New Haven. 274 pp.

Ronen, A., Tsatskin, A., 1995. New interpretation of the oldest part of the Tabun Cave sequence, Mount Carmel, Israel. In: Ulrich, H. (Ed.), Man and Environment in the Palaeolithic. E.R.A.U.L, vol. 62, pp. 265–281.

Sass, E., Bein, A., 1978. Platform carbonates and reefs in the Judean Hills, Carmel and Galilee. Tenth International Congress on Sedimentology. International Association of sedimentologists, Jerusalem, pp. 239–274.

Shahack-Gross, R., Berna, F., Karkanas, P., Weiner, S., 2004. Bat guano and preservation of archaeological remains in cave sites. Journal of Archaeological Science 31, 1259–1272.

White, W.B., White, E.L., 2000. Breakdown morphology. In: Klimchouk, A., Ford, D.C., Palmer, A.N., Dreybrodt, W. (Eds.), Speleogenesis Evolution of Karst Aquifers. National Speleological Society, Huntsville, USA, pp. 427–429.

Yaalon, D.H., Ganor, E., 1973. The influence of dust on soils during the Quaternary. Soil Science 116, 146–155.

Zviely, D., Ronen, A., 2004. Garrod's spring in Tabun Cave, Mt. Carmel (Israel): 70 years later. In: Maos, J.O., Inbar, M., Shmueli, D.F. (Eds.), Contemporary Israeli Geography, Special Issue of Horizons in Geography 60–61. University of Haifa, Haifa, pp. 247–254.